

## Structural and low frequency dielectric studies of conducting polymer nanocomposites

D K Ray\*, A K Himanshu<sup>#</sup> & T P Sinha<sup>+</sup>

<sup>+</sup> Department of Physics, Bose Institute, 93/1, Acharya Prafulla Chandra Road, Kolkata 700 009

<sup>#</sup> Variable Energy Cyclotron Centre, Material Science Section, DAE, 1/AF Bidhan Nagar Kolkata 700 064

\*Department of Radiotherapy, Chittaranjan National Cancer Institute, 37, S P Mukherjee Road, Kolkata 700 026

*Received 14 June 2006; accepted 18 May 2007*

The intrinsically conducting polymer (ICP), polyaniline (PANI) has been synthesized by chemical polymerization process with the help of water soluble support polymer poly (vinyl pyrrolidone) (PVP). The X-ray diffraction of synthesized PANI-PVP polymer reveals that the polymeric nanocomposites are partially crystalline with orthorhombic phase at room temperature. The morphology of these composite polymers has been studied by Transmission Electron Microscopy (TEM) and Scanning Electron Microscopy (SEM). The dielectric measurement of the sample is performed in the frequency range 100 Hz – 1MHz and temperature range 213-313 K. An analysis of real and imaginary parts of dielectric permittivity and the electric modulus indicate the polydispersive nature of relaxation time as confirmed by Cole-Cole plot of the complex permittivity. The frequency dependence of modulus spectra is found to obey an Arrhenius law with activation energy of 0.07 eV. The frequency dependent electrical data has been analyzed in the framework of the conductivity. These results elucidate that there is an increased coupling among the local dipolar motions (short range order localized motion).

**Keywords:** Polyaniline, Polyvinyl pyrrolidone, Polaron, Bipolaron, Emeraldine-salt, Nanocomposites

**IPC Code:** B82B

### 1 Introduction

The polyaniline (PANI) family of polymers has been the subject of increased investigation because of its electronic properties which can be modified by protonation, giving rise to unusual chemical, optical, electro-chronic, and electrical properties in both insulating and conducting forms<sup>1-3</sup>. Synthesis of polyaniline is commonly performed by chemical oxidative polymerization in an aqueous solution<sup>4</sup>. The method involves distilled water, aniline, a protonic acid, and an oxidizing agent and allows the mixture to react while maintaining the reaction mixture to a constant low temperature normally about 5°C. After a period of several hours, the conducting emeraldine salt of polyaniline precipitates. Material synthesized by this approach is predominantly amorphous, intractable, and insoluble in the most organic solvents<sup>4</sup>. Thus, PANI has not yet met its requirements for a wide range of commercial applications. It was an important goal in basic research and application oriented material science to develop techniques by which PANI etc. could be processed easily because of its role as the electrically conducting polymer. Recent reports reveal that the

processability of the PANI can be readily improved by increasing its solubility in organic solvents. PANI dispersion has been prepared by polymerization of pure aniline in micelles<sup>5</sup>, emulsion<sup>6,7</sup>, steric stabilizer<sup>8</sup>, etc. The aniline monomers were dissolved in the reaction medium (distilled water) containing steric stabilizer. The polymerization has been started by addition of initiator such as ammonium peroxodisulphate (APS), and the polymer PANI dispersion was obtained. The macroscopic precipitation of polymer is prevented by the presence of the steric stabilizer<sup>9</sup> such as poly<sup>9</sup> (vinyl alcohol) (PVA), poly<sup>10</sup> (vinyl pyrrolidone) (PVP), poly<sup>11</sup> (vinyl methyl ether), cellulose ethers<sup>12</sup>, etc.

Little is known about the dielectric properties of conducting polymers associated with the conducting mechanism<sup>13-15</sup>. The charge transport mechanism of conducting polymer has been investigated in recent years using dielectric relaxation behaviour and *ac* measurements; etc<sup>16-18</sup>. Low frequency conductivity and dielectric relaxation measurements especially have proven to be valuable in giving additional information on the conduction mechanism as the *dc* conductivity measurement alone does not provide.

The relaxation of an electric field in a charge carrier system is attributable to the charge hopping of mobile carriers, which can lead to both short-range (or local) *ac* conductivity and long-range *dc* conductivity. We have analysed the experimental data by means of two different formalism complex permittivity  $\epsilon^*$  and complex electric modulus  $M^*$ . Transformation from one formalism to another may help to study particulars aspects of the electrical and dielectrical behaviour. Recently, we have studied the electrical properties of PANI synthesized using a water-soluble support polymer<sup>19</sup> PVA. The electrical properties using alternating current impedance spectroscopy (ACIS) of PANI synthesized with the help of another water-soluble support polymer poly (vinyl pyrrolidone) (PVP), have been reported.

## 2 Experimental Details

PANI-PVP (0.05 ml) was chemically synthesized by the *in-situ* polymerization of aniline in 1N aqueous acidic (HCl) medium by using water soluble support polymer: poly (vinyl pyrrolidone) (PVP) and ammonium peroxodisulphate  $[(\text{NH}_4)_2\text{S}_2\text{O}_8]$  (E Merck, India) as the oxidant<sup>10</sup>. The dark green coloured stable aqueous polymer solution was readily obtained for 0.05 ml concentration of aniline. From the green PANI finely dispersed in aqueous PVP solution, the PANI-PVP composite was isolated by co-

precipitation using excess acetone. Isolated green composite mass was dried under vacuum and pelletized.

The X-ray diffraction of the powder of the sample was taken at room temperature using a Philips PW 1877 automatic X-ray powder diffractometer. The shape and size of the particles of the samples were taken by Transmission Electron Microscopy (TEM) (model JEOL-2000). The topographical details of the surface of the specimen were measured using JEOL Scanning Electron Microscopy (SEM). For the dielectrical characterization, the pellet was coated with silver paint. The temperature and frequency dependence of the capacitance and loss tangent of the sample were measured using an LCR meter in our laboratory, in the frequency range 50 Hz-1 MHz and temperature range 213-313 K. The temperature was controlled with the help of a programmable oven. All the electrical data were collected while heating at a rate of  $0.4^\circ\text{C min}^{-1}$ . These results were found to be reproducible.

## 3 Results and Discussion

Figure 1 shows the X-ray diffraction pattern of the PANI-PVP taken at room temperature. The *d* spacings deduced from the angular position  $2\theta$  of the observed peaks, according to the Bragg formula:

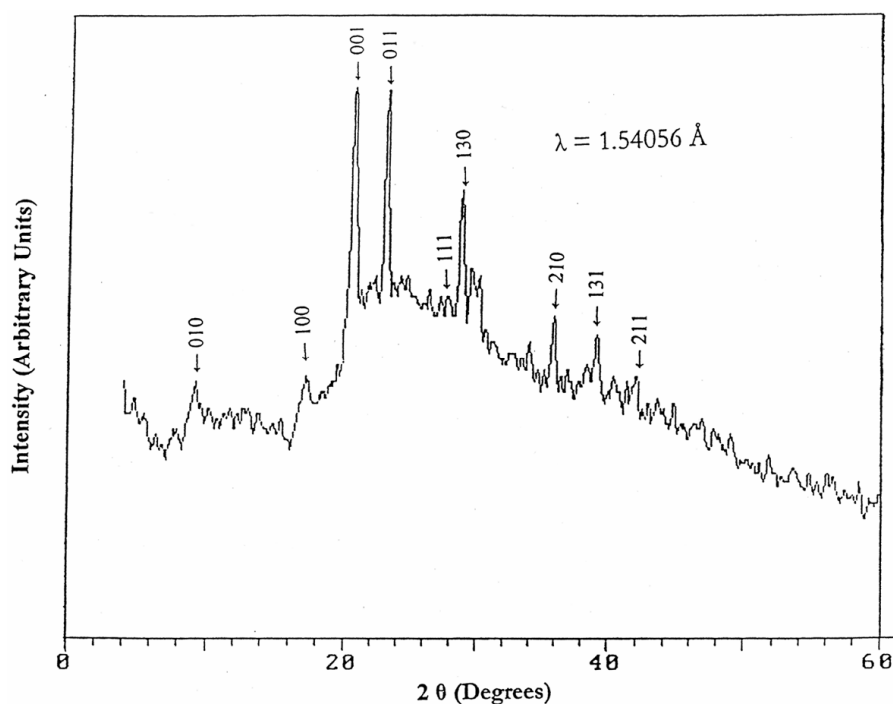


Fig. 1—X-ray diffraction for PANI-PVP

Table 1—X-ray diffraction data for PANI-PVP (5%)

$2\theta$	$d, \text{\AA}$	$hkl$
9.040	9.7743	010
17.035	5.2007	100
20.780	4.2711	001
23.150	3.8389	011
28.620	3.1164	111
29.665	3.0090	130
35.820	2.5048	210
38.980	2.3087	131
41.890	2.1548	211

$$\lambda = 2d\sin\theta \quad \dots (1)$$

are given in Table 1 ( $\lambda$  is the X-ray wavelength used). All the reflections peaks of the X-ray profiles were indexed in a pseudo-orthorhombic cell and lattice parameters were determined using a least-squares method with the help of a standard computer program (POWD). Good agreement between the observed and calculated interplanar planar spacing ( $d$ -values) suggests that the compounds are having orthorhombic structure with  $\alpha = \beta = \gamma = 90^\circ$  ( $a=5.2007\text{\AA}$ ,  $b=9.7743\text{\AA}$ ,  $c= 4.2711\text{\AA}$ , and  $V=217.11 \text{\AA}^3$ ). X-ray diffraction confirms that the specimen is single phase and matches with earlier reported work<sup>1</sup>. A TEM micrograph of nearly 5% PANI shows the presence of discretely dispersed PANI micro-particles of different sizes and shapes in the solution of the support polymer (PVP) in a reasonable uniform distribution (Fig. 2). The morphology of the PVP-supported PANI microparticles (50-150 nm) varies from finer grain-like morphology to somewhat larger spherical or oblong morphology. The observed morphology for aqueous PANI-PVP system combines the characteristic rice grain morphology for PANI prepared in dispersion with the support of such water soluble polymers. The Scanning Electron Micrographs (SEM) of PANI-PVP components (5% PANI loading) is shown in Figure 3. The halo, isotropic morphology of PANI-PVP composites arises due to solubilization of the PANI formed by PVP via strong intermolecular H-bonding and presumably due to limited grafting of PANI formed in addition during the polymerization of aniline.

Figure 4 shows the frequency dependence of the real ( $\epsilon'$ ) and imaginary part ( $\epsilon''$ ) of the dielectric permittivity and loss tangent ( $\tan\delta$ ) in the temperature range 213-313 K. The high values of  $\epsilon'$  and  $\epsilon''$  and  $\tan\delta$  at frequencies lower than 1 kHz increase with

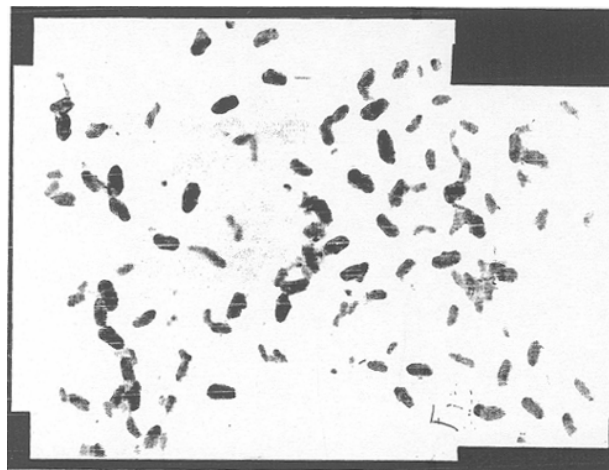


Fig. 2—Transmission electron micrograph of PANI-PVP composites containing 5% PANI

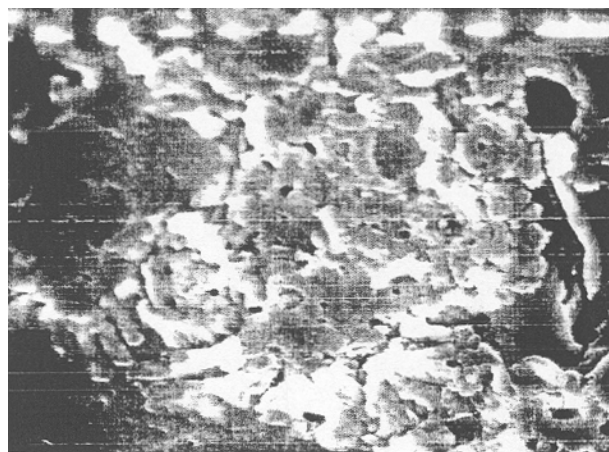


Fig. 3—Scanning electron micrograph of PANI-PVP composites

decreasing frequency and increasing temperature, may be attributable to free charge build up at the interface between the sample and the electrode (space-charge polarization). Figure 5 shows the gradual increase of  $\epsilon'(T)$ ,  $\epsilon''(T)$  and  $\tan\delta(T)$  at low frequencies and higher temperature.

Fig 4(a) shows the frequency dependence of the dielectric permittivity  $\epsilon'$  of PANI-PVP in the temperature range 213-313 K. The magnitude of  $\epsilon'$  decreases with increasing frequencies, which is a typical characteristic of disordered conducting polymer and consistent with the earlier studies<sup>20-22</sup>. The Debye formula giving the complex permittivity related to free dipole oscillating in an alternating field<sup>23</sup> is given as :

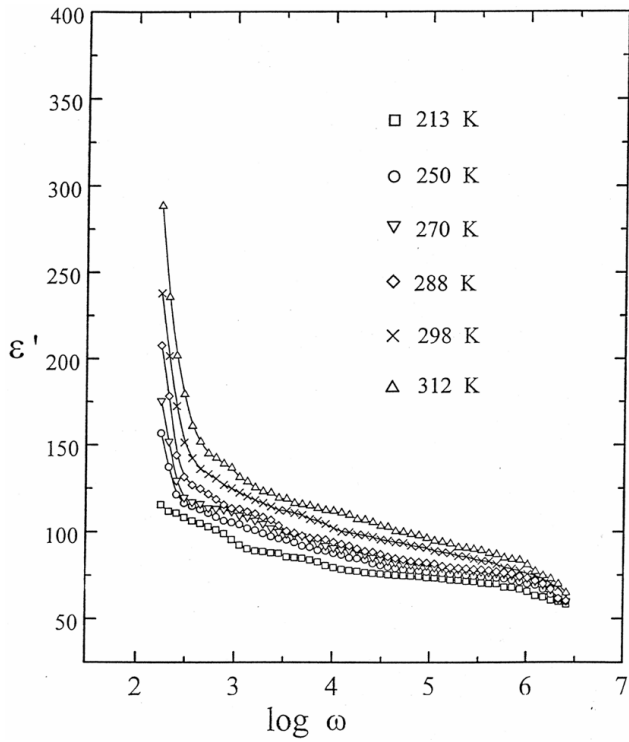


Fig. 4(a)—Frequency dependence of  $\epsilon'$  of PANI -PVP

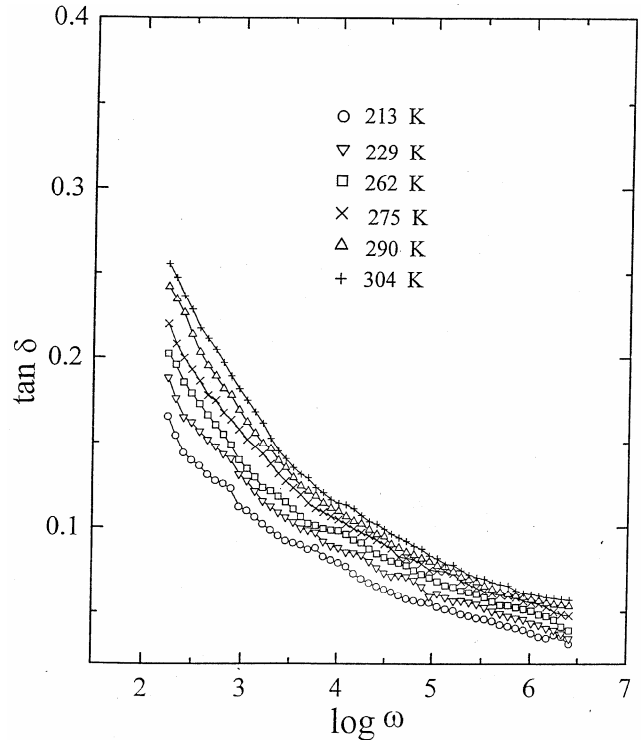


Fig. 4(c)—Frequency dependence of  $\tan \delta$  of PANI -PVP

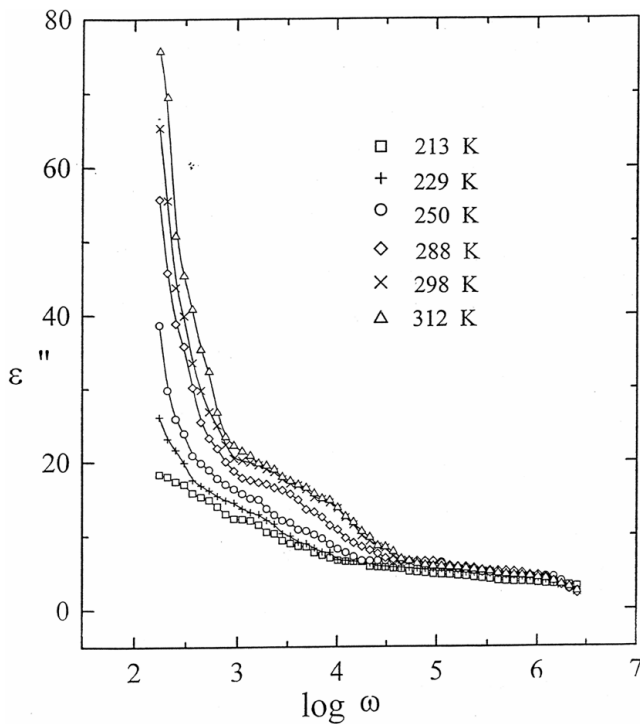


Fig. 4(b)—Frequency dependence of  $\epsilon''$  of PANI -PVP

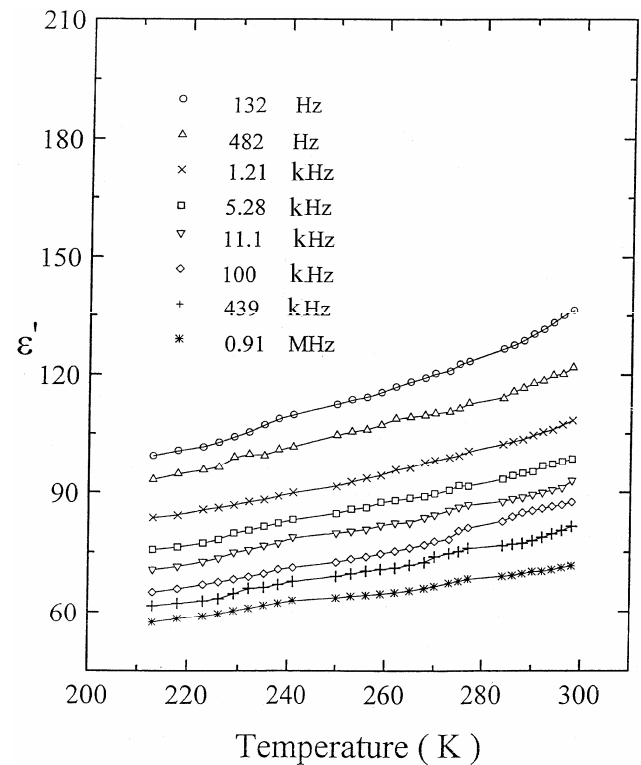


Fig. 5(a)—Temperature dependence of  $\epsilon'$  of PANI -PVP

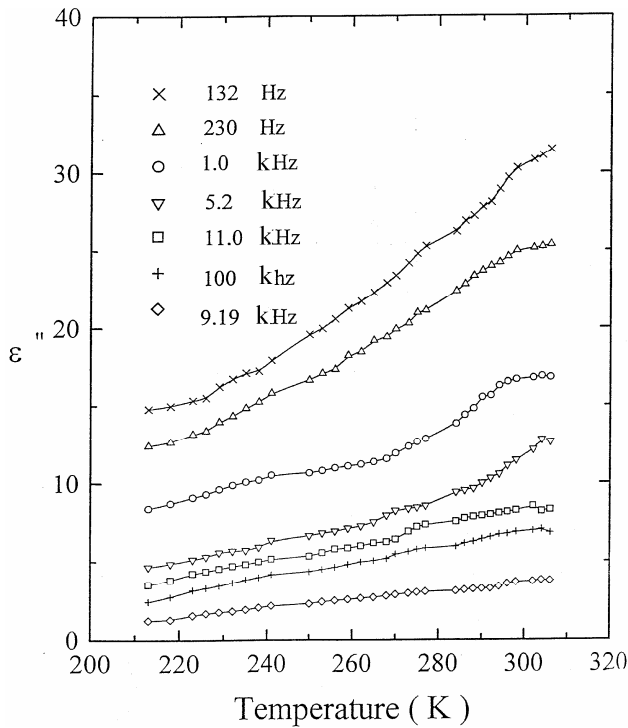


Fig. 5(b)—Temperature dependence of  $\epsilon''$  of PANI-PVP

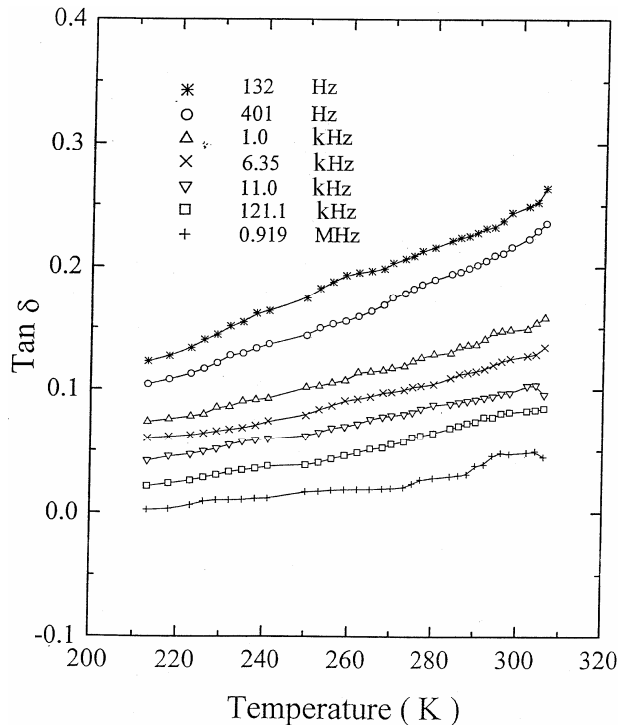


Fig. 5(c)—Temperature dependence of  $\tan \delta$  of PANI -PVP

$$\epsilon^* = \epsilon' - j\epsilon'' = \epsilon_\infty + \frac{(\epsilon_s - \epsilon_\infty)}{1 + j\omega\tau} \quad \dots (2)$$

The real part of  $\epsilon^*$  is :

$$\epsilon' = \epsilon_\infty + \frac{\epsilon_s - \epsilon_\infty}{1 + \omega^2\tau^2} \quad \dots (3)$$

and the imaginary part of  $\epsilon^*$  is :

$$\epsilon'' = (\epsilon_s - \epsilon_\infty) \frac{\omega\tau}{1 + \omega^2\tau^2} \quad \dots (4)$$

where  $\epsilon_s$  and  $\epsilon_\infty$  are the low and high frequency values of  $\epsilon'(\omega)$ ,  $\omega = 2\pi f$ ,  $f$  being the measuring frequency,  $\tau$  is the relaxation time. At higher temperature (HT), the dielectric constant for the highest frequencies approaches the dielectric constant for low temperature (LT) dielectric constant while at lower frequencies (LF) there is an increasing contribution to the dielectric constant. At very low frequencies ( $\omega \ll 1/\tau$ ), dipoles follow the field and we have  $\epsilon' \approx \epsilon_s$  (value of the dielectric constant at quasi-static fields). As the frequency increases (with  $\omega < 1/\tau$ ), dipoles begin to lag behind the field and  $\epsilon'$  slightly decreases. When frequency reaches the characteristic frequency ( $\omega = 1/\tau$ ), the dielectric constant drops (relaxation process). At very high frequencies ( $\omega \gg 1/\tau$ ), dipoles can no longer follow the field and  $\epsilon' \approx \epsilon_\infty$ . Qualitatively, this is the behaviour observed in Fig. 4(a) and the experimental results of Fig. 4(a) confirm the Eq. (3). Even at lower frequencies and higher temperatures, there is a substantial increase in the dielectric constant that is attributable to a dipolar contribution to  $\epsilon'(\omega)$  from the hopping of electrons between isolated polarons and bipolarons state. Electrical conductivity effects give rise to higher values of  $\epsilon''(\omega)$  in Fig. 4(b), increasing with the increasing temperature and decreasing frequency. The high values of  $\epsilon''(\omega)$  at LF/HT are due to the frequent charge motion within the sample<sup>24</sup>.

A relation exists between  $\sigma_{ac}$  and  $\epsilon''$ , given as  $\sigma_{ac} = \epsilon_0\omega\epsilon''$  where  $\sigma_{ac}$  is the *ac* conductivity,  $\omega = 2\pi f$  ( $f$  is the measuring frequency) and  $\epsilon_0$  is the free space permittivity. Moreover, the value of  $\sigma_{ac}$  in Fig. 6 decreases with decreasing frequency at very low frequencies and high temperatures, these drops in  $\sigma_{ac}$  indicate space charge polarization and electrode

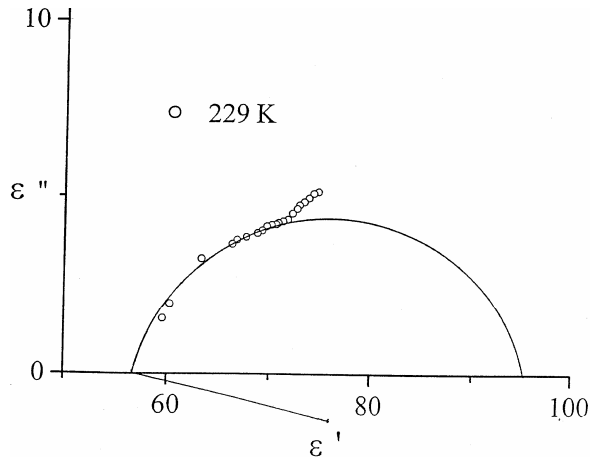


Fig. 6—Cole-Cole plot at temperature 229 K for PANI-PVP

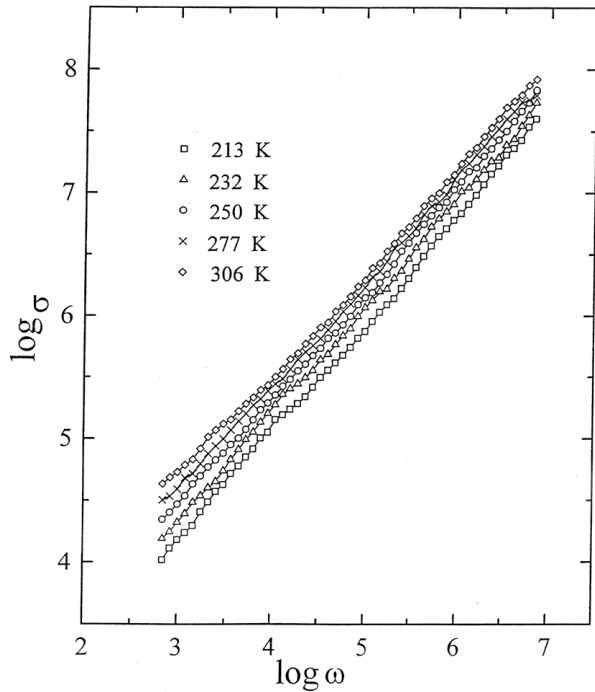


Fig. 7—Frequency spectra of the conductivity for PANI-PVP at various temperatures

polarization<sup>25</sup>. The data analysis of  $\sigma_{ac}$ ,  $\epsilon'(\omega)$  for PANI-PVP show that the charge transport does not occur via the usual mechanisms attributable to insulating materials. The analysis of these data in the context of other data for the PANI-PVP polymer composites supports the possibilities of a new mechanism among fixed polaron site.

The complex dielectric data as shown in Fig. 4(a and b), are shown in Figure 7 in the  $\epsilon''(\omega)$  versus  $\epsilon'(\omega)$  representation. One standard way to analyse the

experimental data is to fit to the Cole-Cole expression<sup>26</sup> :

$$\epsilon^* = \epsilon_\infty + \frac{\Delta\epsilon}{1+(i\omega\tau)^{1-\alpha}} \quad \dots (5)$$

where  $\Delta\epsilon = \epsilon_s - \epsilon_\infty$  is the dielectric relaxation strength and  $\alpha$  is the parameter describing the distribution of the relaxation times. Figure 7 depicts a plot of  $T = 229$  K. It is apparent from the plot that the relaxation process differs from the mono dispersive Debye process (for which  $\alpha = 0$ ). The parameter  $\alpha$  as determined from the angle subtended by the radius of the circle with the  $\epsilon'$ -axis passing through origin of  $\epsilon''$ -axis is 0.155. The value of  $\alpha$  between 0 and 1 ( $0 < \alpha < 1$ ) indicates broad distribution of relaxation times in the system<sup>27</sup>. The Cole-Cole plot confirms the polydisperse nature of the dielectric relaxation time of PANI-PVP.

To analyze the conductivity relaxation properly in depth, the complex permittivity ( $\epsilon^*$ ) is converted to the complex electric modulus  $M^*(\omega)$ , because  $\epsilon^*$  is not completely suitable to describe the electrical properties of the conjugated polymers. The real and imaginary part of  $M^*(\omega)$  can be calculated from  $\epsilon^*(\omega)$  as follows:

$$M^*(\omega) = \frac{1}{\epsilon^*(\omega)} = M' + jM'' \quad \dots (6)$$

the real part of  $M^*(\omega)$  is given as

$$M' = \frac{\epsilon'}{\epsilon'^2 + \epsilon''^2} \quad \dots (7)$$

and the imaginary part of the  $M^*(\omega)$  is given as

$$M'' = \frac{\epsilon''}{\epsilon'^2 + \epsilon''^2} \quad \dots (8)$$

Figure 8(a and b) shows the frequency dependence of  $M'(\omega)$  and  $M''(\omega)$  as a function of temperature.  $M'(\omega)$  shows a dispersion tending towards  $M_\infty$  (the asymptotic value of  $M'(\omega)$  at higher frequencies [Fig.8(a)]) and that  $M'(\omega)$  approaches to zero at low frequencies, indicating that the electrode polarization gives a negligible low contribution to  $M'(\omega)$  and being ignored when the permittivity data are expressed in this form<sup>28</sup>. Figure 8(b) shows the frequency dependence of the imaginary part of electric modulus

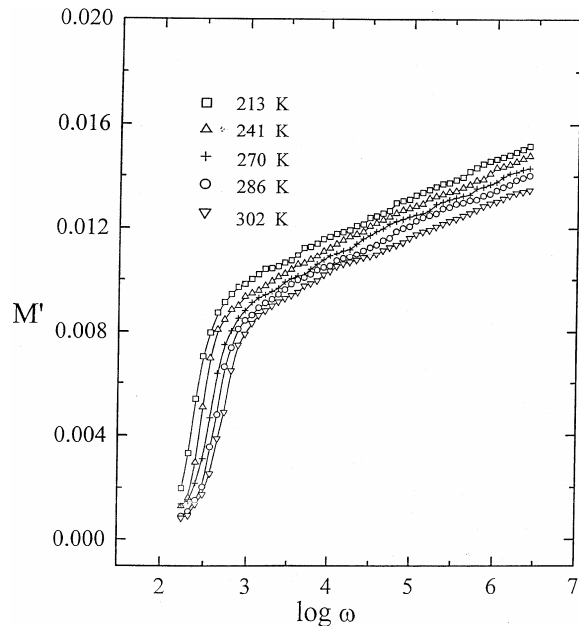


Fig. 8(a)—Frequency dependence of  $M'$  of PANI-PVP at various temperatures

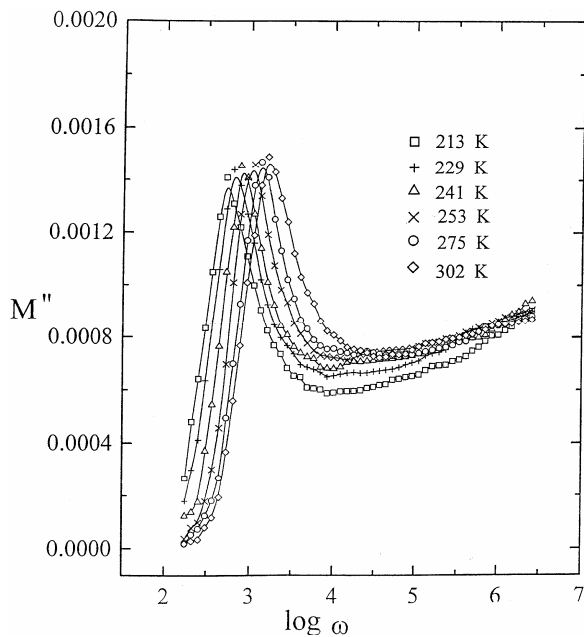


Fig. 8(b)—Frequency dependence of  $M''$  of PANI-PVP at various temperatures

of the PANI-PVP composites. A peak is observed which shifts to higher frequencies with the increasing temperature. The frequency  $f_{max}$  of the peak is assumed to represent a characteristic frequency of the conductivity relaxation. It defines the conductivity

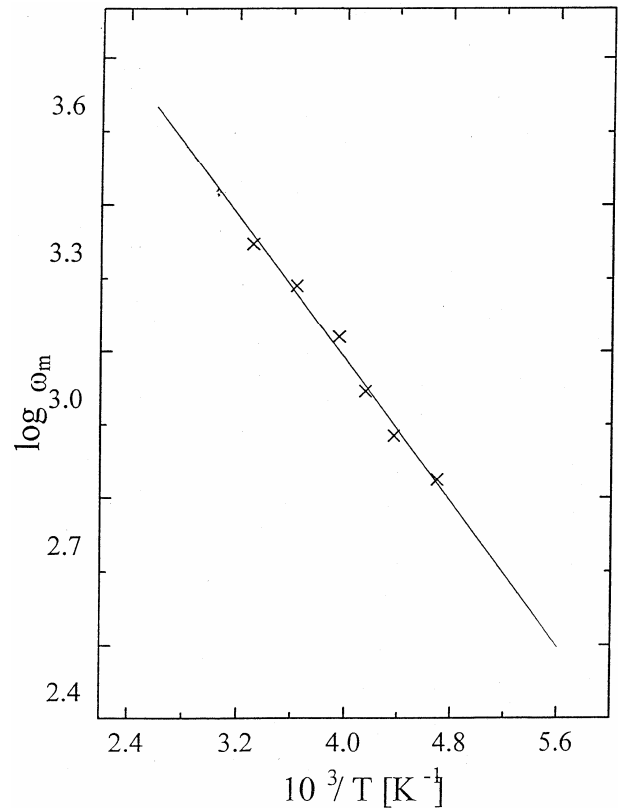


Fig. 9—Temperature dependence of the most probable relaxation frequency obtained from the impedance formalism for PANI. The crosses are the experimental points and the solid line is the least-squares straight-line fit

relaxation time by  $2\pi f_{max}=1$  a measure for the conductivity relaxation time,  $\tau$ , which is assumed to represent a characteristic time scale of the ionic motion<sup>29</sup>.

The frequency ( $\omega_m$ ) corresponding to  $M''_{max}$  gives the most probable relaxation time  $\tau_m (=1/\omega_m)$ . The most probable relaxation time obeys the Arrhenius relation given by as follows:

$$\omega_m = \omega_0 \exp\left[\frac{-E_a}{k_B T}\right] \quad \dots (9)$$

where  $\omega_0$  is the pre-exponential factor  $k_B$  is the Boltzmann's constant and  $T$  is the absolute temperature and  $E_a$  is activation energy. Fig. 9 shows a plot of  $\log \omega_m$  versus  $1/T$ , where the crosses are the experimental data. The activation energy  $E_a$  calculated from least squares fit to the data points is 0.07 eV. We have also scaled each  $M''(\omega)$  by  $M''_{max}$  and each

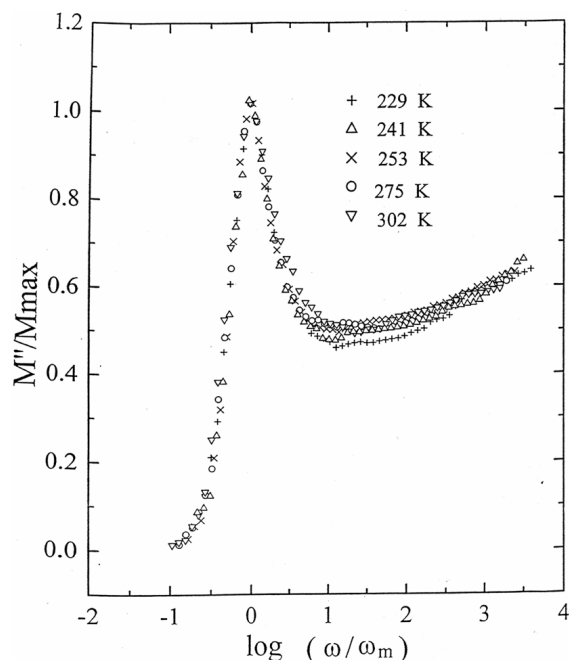


Fig. 10—Scaling behaviour of  $M''$  at various temperatures for PANI-PVP

angular frequency by  $\omega_m$  for different temperature as shown in the Figure 10, the very good overlap of the different temperature data for  $M''(\omega)$  suggests that the dynamical process occurring at different frequencies exhibits the same activation energy, so that a distribution of activation energies should not be considered as the origin of the non-exponential response<sup>30</sup>.

#### 4 Conclusion

PANI-PVP synthesized by oxidative polymerization has been investigated. The X-ray diffraction of the sample at room temperature reveals that the polymeric nanocomposites are crystalline with orthorhombic phase. The TEM micrograph of PVP supported PANI microparticles (50-150 nm) vary from finer grain like morphology to somewhat spherical or oblong morphology. The SEM micrograph of PANI-PVP shows the halo, isotropic morphology. Analysis of the real and imaginary parts of the dielectric permittivity and electric modulus were performed, showing the polydispersive nature of relaxation time as confirmed by Cole-Cole plot complex permittivity as well as the scaling behaviour of the modulus spectra. The frequency dependence of the modulus spectra is found to obey Arrhenius law with activation energy of 0.07 eV. The existence of the master curve for the modulus spectra implies that

the shape of the relaxation spectrum does not change with temperature. These results clearly suggest that there is an increased coupling among the dipolar motion (short range order localized motion).

#### References

- 1 Pouget J P, Jozefowicz M E, Epstein A J, Tang X & MacDiarmid A G, *Macromolecules*, 24 (1991) 779.
- 2 Baughman R H, Wolf J F, Eckhardt H & Shacklette L W, *Synth Met*, 25 (1988) 121.
- 3 Heeger A J, *Faraday Discuss Chem Soc*, 88 (1989) 1.
- 4 Cao Y, Andreetta A, Heeger A J & Smith P, *Polymer*, 30 (1989) 2305.
- 5 Kuramoto N & Genies E M, *Synth Met*, 68 (1995) 191.
- 6 Kinlen P J, Liu J, Ding Y, Graham C R & Remsen E E, *Macromolecules*, 31 (1998) 1735.
- 7 Osterholm J E, Cao Y, Klavetter F & Smith P, *Synth Met*, 55 (1993) 1034.
- 8 Riede A, Helmstedt M, Riede V & J Stejskal, *Langmuir* 14 (1998) 6767.
- 9 Ray D K, Roy R K, Roy B & Sinha T P, *J Acous Soc Ind*, 28 (2000) 289.
- 10 Himanshu A K, *M Phil dissertation*, Jiwaji University, India, 2003.
- 11 Banarjee P, Bhattacharya S N & Mandal B M, *Langmuir*, 11 (1995) 2414.
- 12 Chattopadhyay D, Banarjee S, Chakravorty D & Mandal B M, *Langmuir*, 14 (1998) 1544.
- 13 Singh R, Arora V, Tandon R P, Mansingh A & Chandra S, *Synth Met*, 104 (1999) 137.
- 14 Zuo F, Angelopolous M, MacDiarmid A G & Epstein A J, *Phys Rev B*, 39 (1989) 3570.
- 15 Singh R, Narula A K & Tondon R P, *Synth Met*, 82 (1996) 245.
- 16 Capaccioli S, Lucchesi M, Rolla P A & Ruggeri G, *J Phys : Condens Matter*, 10 (1998) 5595.
- 17 Ram M K, Annapoorni S, Pandey S S & Malhotra B D, *Polymer*, 39 (1998) 3399.
- 18 Moon G H & Seung I S, *J Appl Polym Sci*, 82 (2001) 2760.
- 19 Ray D K, Himanshu A K & Sinha T P, *Indian J Pure & Appl Phys*, 43 (2005) 787.
- 20 Himanshu A K, Ray D K & Sinha T P, *Indian J Phys*, 79 (2005) 1049.
- 21 Matteeva E S, *Synth Met*, 79 (1996) 127.
- 22 Lian A, Besner S & Dao L H, *Synth Met*, 74 (1995) 21.
- 23 Bottcher C F S & Bordewijk P, *Theory of Electric Polarization*, 2<sup>nd</sup> Ed El-Seiver Amsterdam, 1998.
- 24 Hedvig P, *Dielectric Spectroscopy in Polymers*, Adam Hilger, Bristol, 1977 p 283.
- 25 Raistrick I D, in *Impedance Spectroscopy*, edited by I R Macdonald Wiley, New York, 1987, Chap 2.
- 26 Cole R S & Cole R H, *J Chem Phys*, 9 (1941) 341.
- 27 McCrum N G, Read B E & Williams G, *Anelastic & Dielectric Effects in Polymeric Solids* (Wiley, New York), 1967, p 478.
- 28 Lee H T, Lio C S & Chen S A, *Macromol Chem*, 194 (1993) 2433.
- 29 Jonscher A K, *Dielectric Relaxation in Solids*, Chelsea Dielectrics Press, London, 1983.
- 30 Zouari N, Mnif M, Khemakhem H, Mhiri T & Daoud A, *Solid State Ionics*, 110 (1998) 269.